2009 American Control Conference
Hyatt Regency Riverfront, St. Louis, MO, USA
June 10-12, 2009

Tip-Over Stability Analysis of Mobile Boom Cranes with Double-Pendulum Payloads

Daichi D. Fujioka, Andreas Rauch, William E. Singhose
Georgia Institute of Technology

Taft Jones
Georgia Southern University

Abstract— **Mobile boom cranes are used throughout the world to perform important and dangerous manipulation tasks. The usefulness of these cranes is greatly improved if they can utilize their mobile base during the lifting and transferring phases of operation. During such operations, the tip-over stability is degraded when the payload swings. This paper presents a stability study of such cranes with payloads that cause double-pendulum dynamics. As a first step, a static stability analysis of a single-pendulum boom crane is conducted to provide basic insights into the effects of the payload weight and crane configuration. Then, a semi-dynamic method is used to take the payload swing into account. Finally, the results of a dynamic stability analysis obtained by using a full dynamic multi-body simulation are compared to the outcomes of the previous approaches. The results of the semi-dynamic method and the full dynamic simulation are verified by experiments. This analysis provides useful guidance for the practical tip-over stability analysis of mobile boom cranes and motivates the need to control payload oscillations.**

I. INTRODUCTION

Cranes attached to fixed bases are widely used for heavy lifting in various applications. However, their productivity is limited because their workspace is constrained in size. Moving the base of the crane during lifting operations can enhance the productivity tremendously, but this poses a stability hazard. The tip-over problem is of concern with mobile booms cranes, cherry pickers, lifting trucks, aerial platforms, and vehicles of a similar type. The rollover problem is also critical in the design of All Terrain Vehicles (ATVs) and Sport Utility Vehicles (SUVs) [1]. Previous investigations in the area suggest methods to prevent rollover by limiting the maximum lifting speed [2]. To predict rollover situations, complex dynamic models including wheel slip, tire stiffness, as well as lateral load transfer were developed [3].

Several investigations into the tip-over stability of cranes have also been performed. However, most of the previous work limited their investigations to a fixed base location during crane operation. Towarek studied the dynamic stability of a boom crane on a flexible soil foundation [4]. Kilicaslan, Balkan, and Ider calculated the maximum possible payload a mobile crane can carry and move while its base and stabilizing arms are kept fixed [5].

Another factor that significantly impacts the crane stability is payload oscillations. Payload swing due to base excitation motion was studied, and a technique limiting these oscillations by reeling and unreeling the hoisting cable was developed [6]. The anti-sway problem was investigated and formulated as a nonlinear constrained optimal control problem [7]. Lewis, Parker, Driessen and Robinett developed a method to reduce payload oscillation by utilizing adaptive command filters [8]. Certain types of payloads and riggings can induce double-pendulum effects that increase the complexity of the problem [9], [10], [11], [12].

In this paper, the tip-over stability of mobile boom cranes carrying double-pendulum payloads is investigated. First, a static stability analysis of a simple mobile boom crane is conducted to provide insights into the relationship between the crane configuration and the maximum allowable payload. Then, the analysis is extended to a semi-dynamic method by including the influences from payload swing angles. This analysis is used to investigate the crane's behavior during simple base maneuvers. A full dynamic multi-body simulation of the crane is then created to better analyze the crane's behavior, and the results are compared with those of the semi-dynamic analysis. Experiments are performed to verify the simulated results. The results indicate that payload oscillation can significantly compromise crane tip-over stability.

II. DOUBLE-PENDULUM MOBILE BOOM CRANE MODEL

To investigate mobile boom crane stability, a representative model of a crane was developed. Figure 1 shows the model utilized for the static analysis. The model is composed of a cart platform with tires, a rotational boom, and cables with end point masses. The cart is modeled as a thin plate, and has a mass of m_c and a center of gravity at distances of l_{com} and b_{com} away from it geometric center. The boom can rotate through an angle β about a point located at a distance l_a forward of the cart's geometric center. The boom is mounted on top of the rotational platform at a distance l_{a2} in front of the platform's rotational center. It has a mass of m_b, length of l_b, and a center of mass located at a distance l_{bcom} from the attachment point. The boom can be raised in a luffing motion through angle α.

Four wheels are attached to the bottom of the cart. The wheels are separated by l_c in the longitudinal direction, and b_c in the lateral direction. The suspension cables l_1 and l_2 have negligible masses compared to the payloads m_1 and

978-1-4244-4524-0/09/$25.00 ©2009 AACC

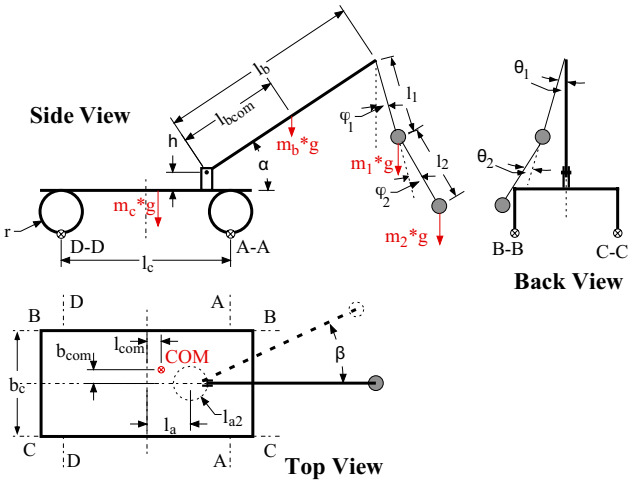

Fig 1. Schematic Diagram of a Mobile Boom Crane

m_2 attached at the end of the cable segments. The payload oscillations of the double-pendulum crane are defined in the longitudinal and the lateral directions with respect to the cart. The angles φ_1 and φ_2 describe the payload oscillation of m_1 and m_2 respectively in the longitudinal direction. Similarly, the angles θ_1 and θ_2 describe the payload oscillation of m_1 and m_2 in the lateral direction to the cart.

A. Static Stability Analysis

A static stability analysis was performed to study the tip-over stability of the mobile boom crane when it is stationary and without payload swing (φ_i and θ_i are zero). The analysis calculated the maximum payload that can be attached to the boom without causing it to tip-over. This analysis was conducted for every possible boom angle configuration. Therefore, the tip-over condition is split into distinct cases: The crane will tip-over either to the front (rollover axis indicated as A-A in Figure 1), to the back (rollover axis indicated as D-D in Figure 1), or to the side (rollover axes indicated as B-B and C-C in Figure 1). Equilibrium conditions for the torques about these axes were formulated. These torque equilibriums consist of contributions from the cart and the boom weight, from the two payload weights, and from the ground contact forces exerted on the wheels. If these contact forces vanish, then the crane is starting to tip-over. For every boom position, the total weight of the payloads that first causes the wheel contact forces to vanish was recorded as the maximum possible payload.

A single-pendulum crane apparatus, shown in Figure 2, was used to experimentally verify the analysis. The geometric parameters and constants for the setup are listed in Table I. To allow a reasonable comparison between the single-pendulum setup and the double-pendulum mobile boom crane model, the cable lengths l_1 and l_2 are adjusted so that the total length was equal to the cable length used in a single-pendulum setup. In addition, the mass m_1 was set to $0kg$.

Figures 3 and 4 show the maximum possible payload plotted against the slew angle, β, for two different values

Fig 2. Single-Pendulum Crane Experimental Apparatus

TABLE I. Geometric Parameters of a Single-Pendulum Crane Apparatus

m_c	$24.9kg$	l_b	$1.70m$
m_b	$8.0kg$	l_{bcom}	$0.80m$
l_c	$1.10m$	l_{com}	$0.12m$
b_c	$0.70m$	b_{com}	$0.0m$
l_a	$0.30m$	r	$0.14m$
l_{a2}	$0.28m$	h	$0.14m$
l	$l_1 + l_2$	m_1	$0kg$

of the luffing angle, α. The solid lines show the predicted values, while the diamonds indicate the experimental results. The maximum payload follows the same trends in both graphs, but on a different scale.

The payload value reaches local minimums at $\beta = 0°$, $90°$, $180°$, and $270°$. The global minimum occurs at $\beta = 90°$ (and $\beta = 270°$) and a luffing angle $\alpha = 0°$. This is when the boom points exactly to the side and reaches out as far as possible. By limiting the payload to the maximum value at this location, a stable static behavior can be guaranteed over the entire workspace.

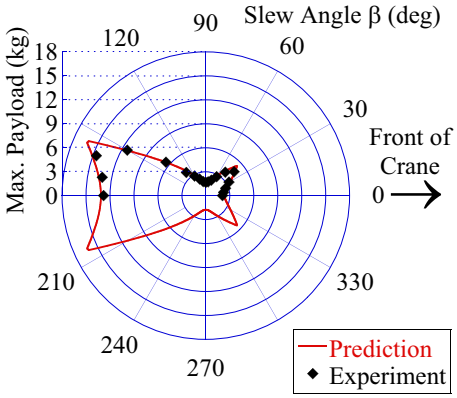

Fig 3. Max. Payload for $\alpha = 0°$ (Static Stability)

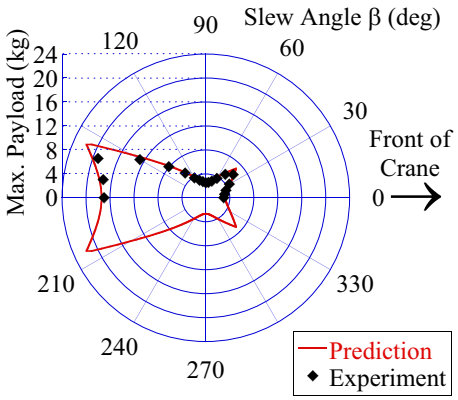

Fig 4. Max. Payload for $\alpha = 30°$ (Static Stability)

B. Single-Pendulum Semi-Dynamic Stability Analysis

Since the goal of this investigation is to develop a practical tip-over stability analysis method for mobile boom cranes, the static stability analysis is extended to a semi-dynamic stability analysis by including payload swing angles in the torque calculation. This is critical to the analysis because large payload swings can dramatically decrease the crane stability. The swing angles, φ_i and θ_i in Figure 1, are still regarded as static in this analysis, *i.e.* the payloads are deflected, but remain statically in the deflected position. The magnitude of the swing angle from a worst-case swing condition due to a straight-line driving maneuver is used to conduct the stability analysis.

To calculate the maximum swing angle, a closed-form solution based on the acceleration command is derived. The equation of motion for a one-dimensional, undamped single-pendulum with an accelerating suspension point is investigated. The dynamic behavior of such a pendulum is governed by:

$$\ddot{\varphi}(t) + \omega^2 \sin\varphi(t) = -\frac{d^2x(t)/l}{dt^2}\cos\varphi(t) \tag{1}$$

where φ is the swing angle, ω is the natural frequency of the pendulum, and x is the position of the suspension point. Using the small angle approximation for φ ($\varphi \ll 1 \Rightarrow \sin\varphi \approx \varphi, \cos\varphi \approx 1$), the equation can be linearized and transformed into the Laplace domain.

$$G(s) = \frac{\Phi(s)}{A(s)} = -\frac{1}{l(s^2+\omega^2)} \tag{2}$$

where $A(s)$ is the Laplace transform of the suspension point acceleration.

In this investigation, the acceleration command is limited to bang-coast-bang commands (trapezoidal velocity commands). In the Laplace domain, such a command can be described as:

$$A(s) = \frac{M}{s}(1 - e^{-T_2 s} - e^{-T_3 s} + e^{-T_4 s}) \tag{3}$$

where M is the magnitude of the acceleration and the $T_i s$ are the respective switch times. Most significant for the investigations of the tip-over stability are the worst cases for the switch times in the command, *i.e.* the switch times that cause the highest amplitude of payload swing. In order to obtain the worst-case swing angle, the resulting expression for $\Phi(s)$ is transformed into the time domain:

$$\begin{aligned}\varphi(t) = -\frac{M}{l\omega^2}\Big(&\big(1-\cos(\omega t)\big) \\ &-\big(1-\cos(\omega(t-T_2))\big)\sigma(t-T_2) \\ &-\big(1-\cos(\omega(t-T_3))\big)\sigma(t-T_3) \\ &+\big(1-\cos(\omega(t-T_4))\big)\sigma(t-T_4)\Big)\end{aligned} \tag{4}$$

It can be deduced from (4) that the largest swing angles occur when the cosine terms are all in phase and the multiplying step functions σ are all equal to 1, which means that $t \geq T_4$. This results in the following expression for the absolute value of the maximum possible swing angle:

$$|\varphi_{max}| = \frac{4M}{g} \tag{5}$$

In order to establish the accuracy of the result, a simulation of a nonlinear single-pendulum was used to obtain the maximum swing under a variety of conditions. Consider the case when the crane is accelerated at a constant rate of $1.0m/s^2$ up to a maximum speed of $1.0m/s$. The deceleration occurs at the same rate as the acceleration, but is negative in value.

The maximum payload swing angles for this maneuver were computed for move distances between three and ten meters. Because the swing angles φ and θ are measured relative to the cart, the boom's position does not matter in this case. By using a payload suspension length l of $1m$, the pendulum has a natural frequency of $\omega = sqrt(\frac{g}{l}) \approx 3.132rad/s$. This means that the first and the second, as well as the third and the fourth cosine terms in (4) combine constructively ($T_2\omega = (T_4 - T_3)\omega = 1s \times 3.132rad/s \approx \pi$). Varying T_3 by using different move distances, the worst-case maneuvers with the largest possible swing angles for these acceleration and velocity limits can be obtained.

Figure 5 shows the maximum swing angles for a suspension length of $1m$ for different maximum speeds and an acceleration of $1m/s^2$. The humps in the curve occur when the first and the second pair of cosine terms in (4) are in phase. According to (5), the maximum swing angle for this maneuver is $0.4077rad$, which agrees with Figure 5. The figure also shows, as predicted, that this maximum swing angle occurs for an acceleration of $1m/s^2$ at a maximum speed of $1m/s$. Because neither the first and the second, nor the third and the fourth cosine terms in (4) are in phase for the other values of v, the maximum possible swing angles caused by these maneuvers are lower.

Another interesting effect that can be seen in Figure 5 is that the maximum swing angle cannot be reduced below $0.2rad$ for values of v greater than or equal to one. This limit occurs because this is the amplitude of deflection caused by the initial acceleration. Only by keeping the acceleration

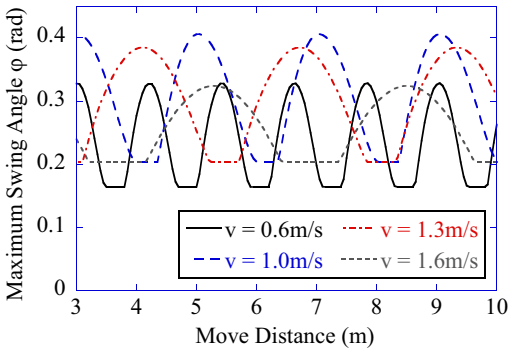

Fig 5. Max. Swing Angles vs. the Moving Distance

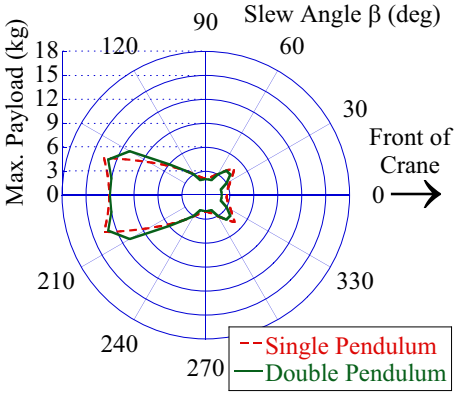

Fig 6. Max. Payload for $\alpha = 30°$ (Semi-Dynamic Stability)

pulse very short, and thus the maximum velocity v very low, it is possible to reduce the maximum vibration below that value, as can also be seen in Figure 5 for $v = 0.6m/s$.

C. Double-Pendulum Semi-Dynamic Stability Analysis

The maximum swing angle calculated for a single-pendulum was directly applied to the double-pendulum stability analysis. This is justified by assuming that the worst case occurs when both cable segments l_1 and l_2 are swung outward to form the same angle with the vertical direction ($\varphi_2 = \theta_2 = 0$). For this reason, the maximum swing angle given by (5) is reused. By setting the magnitude of the acceleration to $1m/s^2$ and the total payload suspension length to $1m$, the maximum swing angle of $0.4077rad$ ($23.36°$) was computed and used for the stability analysis.

The results of the semi-dynamic stability analysis of the mobile boom crane model equipped with single- and double-pendulum were compared. The same parameters from Table I were used for the single-pendulum. For the double-pendulum, the cable lengths l_1 and l_2 were again adjusted to set the total length equal to the cable length used for the single-pendulum. To reduce complexity, equal lengths for l_1 and l_2 were used, and the mass m_1 was set to a fixed value of $1kg$. In Figure 6, the maximum possible payload ($m_1 + m_2$ for the double-pendulum) is plotted against the slew angle β for a fixed luffing angle of $\alpha = 30°$. The plot illustrates that the maximum payload for the single-pendulum and the double-pendulum follow a similar shape. However, some differences arise because the double-pendulum case includes m_1 and the single-pendulum case does not. In some cases m_1 acts as a stabilizing force. However, when m_1 swings out past the wheel base, it acts to decrease the tip-over stability. Also, note that the maximum payload values in Figure 6 are lower than those in Figure 4 (static case), indicating that payload oscillations do make a mobile crane less stable.

A payload deflection was added to the static stability analysis by using the single-pendulum maximum swing angles. In this investigation, the crane was only moved in the forward direction, thus the values for the lateral swing θ were zero. Furthermore, the semi-dynamic analysis does not take the centripetal force caused by the longitudinal swing into account, which also has an influence on the torque equilibrium about rollover axis B-B. In order to compensate

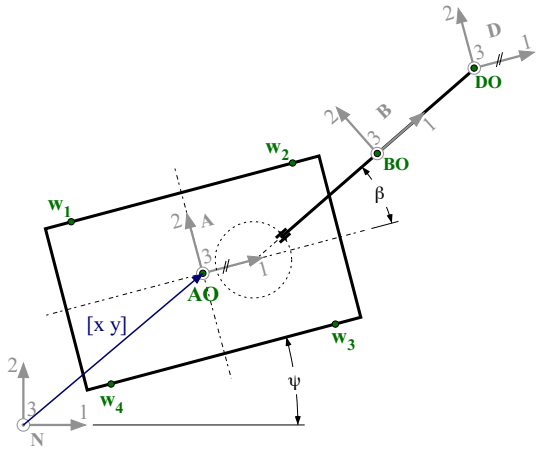

Fig 7. Dynamic Multi-Body Model (Top View)

for this fact, and to make the semi-dynamic estimation more conservative, the longitudinal payload swing φ was also added as a lateral payload deflection. In addition to that effect, the torque about the rollover axis A-A caused by the inertia forces affecting the boom and the cart during the deceleration of the driving maneuver can be added to the torque equilibrium as a constant. This only impacts the forward tipping condition, decreasing the maximum payload near the front of the crane.

III. Dynamic Stability Analysis

A double-pendulum crane can exhibit a rich and complex dynamic behavior that can significantly impact the stability of the mobile platform. Therefore, the full dynamic effects of payload swing angles must be considered. To fully investigate the stability analysis of the double-pendulum mobile boom crane, a dynamic multi-body simulation of the crane was developed.

Figure 7 shows the top view of a schematic model of the multi-body simulation. The origin of the coordinate system **A** is located on the ground. The cart's position in the Newtonian coordinate system **N** is defined by a vector $[xy]$ that describes the location of the origin of **A** and a rotation about a vertical axis (angle ψ). The boom rotates relative to the cart (angle

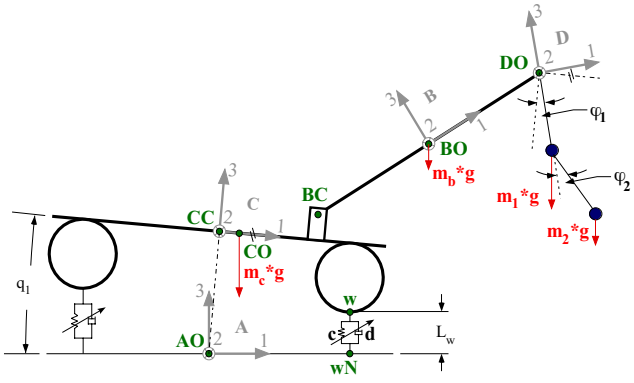

Fig 8. Full Dynamic Multi-Body Simulation Model (Side View)

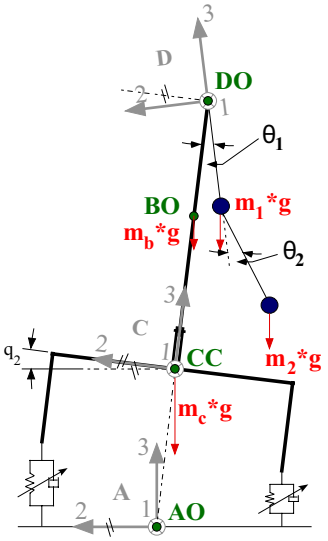

Fig 9. Full Dynamic Multi-Body Simulation Model (Back View)

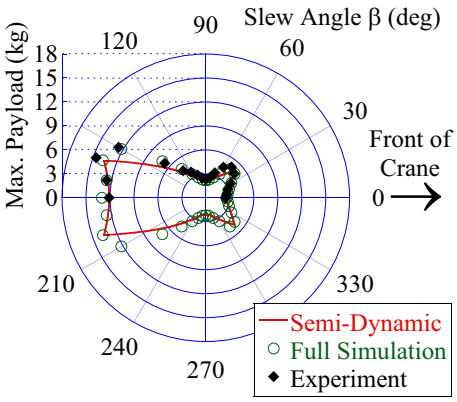

Fig 10. Max. Payload for $\alpha = 30°$ (Semi-Dynamic and Dynamic Stability)

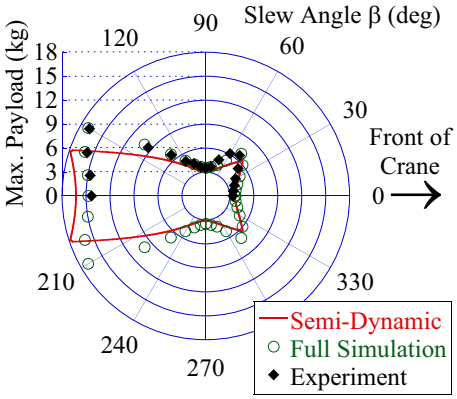

Fig 11. Max. Payload for $\alpha = 45°$ (Semi-Dynamic and Dynamic Stability)

β). The coordinate system **D** is always aligned with **A**. Thus, it is possible to describe the payload swing angles relative to the cart.

Figure 8 shows a side view of the model. The cart can pitch along its lateral axis, described by angle q_1. It can also move up and down. Therefore, the vector from point AO to point CC (indicated as a dotted line in Figure 8) has a variable length, but is always aligned with coordinate system **C**. The cart motion is constrained by wheel-ground contacts, modeled by spring-damper subsystems. To better match the behavior of a real system, these forces are limited to be compressive forces so that the springs do not pull the wheels back to the ground. The payload swing angles are measured relative to the coordinate system **C**. The basic dimensions and weights of the crane are taken from the single-pendulum crane apparatus utilized in the static stability experiment.

Figure 9 shows the model from the back. The location of the center of the cart CC is defined by a vector that is collinear with the upward pointing axis of the coordinate system **C**. The cart rotates relative to the **A** frame about the longitudinal axis of the cart, described by angle q_2.

This multi-body simulation was used to detect the maximum payload that does not cause a bucking motion, *i.e.* the wheels of the crane do not lose contact to the ground at any time, when the maximum swing angle is $0.4077 rad$. A bucking motion does not require any translational movement of the cart. Therefore, no influence of the cart's or boom's inertia caused by acceleration or deceleration was utilized.

Figures 10 and 11 show the results from the full dynamic simulations and the semi-dynamic model prediction, as well as the experimental outcomes for two different values of the luffing angle α. The results from the simulation match up with those from the experiments. Additionally, the semi-dynamic model reproduces the shape obtained by the simulations and experiments. For $\alpha = 30°$ it underestimates the maximum possible payload over the whole range of slew angles β. This is a desirable result because it provides an approximate, yet conservative, estimation. For $\alpha = 45°$, however, the predicted maximum payload lies higher than the results obtained from the simulations and experiments

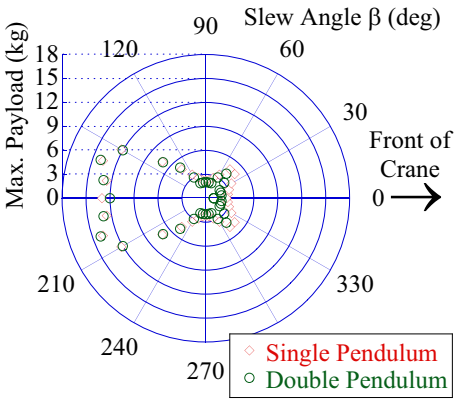

Fig 12. Max. Payload for $\alpha = 30°$ (Dynamic Stability)

around $\beta = 0°$ and $\beta = 180°$. A closer investigation shows that the semi-dynamic model tends to overestimate the maximum stable payload with increasing values of α. Because the maximum payload values for lower values of α are also lower and thus more critical for stability, this effect does not compromise the usefulness of this stability analysis.

Figure 12 illustrates the results of the full dynamic stability analysis of the mobile boom crane model equipped with single- and double-pendulums. The maximum possible payload is plotted against the slew angle β for a fixed value of the luffing angle ($\alpha = 30°$). An arbitrary bang-coast-bang acceleration input of $1.0m/s^2$ with $2.5sec$ intervals between the pulses was supplied to accelerate the cart. The circular markers represent the double-pendulum simulation results, and the diamond markers indicate the single-pendulum simulation results.

Many of the simulated results coincide, especially toward the back of the crane, indicating a similar stability behavior for both single-pendulum and double-pendulum cases. This is beneficial because the semi-dynamic stability analysis, which is a simple and practical tool, also produced results illustrating the similar stability characteristics for both cases.

Figure 12 also shows that the double-pendulum mobile boom crane is less stable than the single-pendulum mobile boom crane. This effect is more apparent toward the front of the crane. This clearly shows that the extra weight and the double-pendulum dynamics hinder the overall stability of a mobile boom crane. The complex swinging motion produced a reduced workspace area, and thus leads to lower crane performance efficiency.

IV. Conclusions

A static stability analysis revealed basic insights into tip-over stability properties of a mobile boom crane. A semi-dynamic model was developed to extend the analysis to account for simple driving maneuvers that induce payload swings and inertia forces. The results from the semi-dynamic analysis align with the outcomes of a full dynamic simulation of the mobile boom crane for low values of the luffing angle. Experiments with a single-pendulum crane apparatus verified the results. Thus, the semi-dynamic model estimation provides a useful and simple tool to investigate the tip-over stability of mobile boom cranes with double-pendulum payloads.

Acknowledgements: The authors would like to thank Siemens Energy and Automation for providing the equipment and funding for this research.

References

[1] Y. Lee and S.-J. Yi, "Rollover prevention for sport utility vehicle using fuzzy logic controller," in *ICMIT 2005: Control Systems and Robotics, Proc. of SPIE*, vol. 6042, 2005.

[2] M. Bertoluzzo, G. Buja, L. Cuogo, G. Sulligoi, and E. Zagatti, "Anti-roll control for by-wire lift truck," in *EUROCON*, Belgrade, Serbia & Montenegro, 2005.

[3] N. Bouton, R. Lenain, B. Thuilot, and J.-C. Fauroux, "A rollover indicator based on the prediction of the load transfer in presence of sliding: application to an all terrain vehicle," in *IEEE International Conference on Robotics and Automation*, Rome, Italy, 2007.

[4] Z. Towarek, "Dynamic stability of a crane standing on soil during the rotation of the boom," *International Journal of Mechanical Sciences*, vol. 40, no. 6, pp. 557–574, 1988.

[5] S. Kilicaslan, T. Balkan, and S. Ider, "Tipping loads of mobile cranes with flexible booms," *Journal of Sound and Vibration*, vol. 223, no. 4212, pp. 645–657, 1999.

[6] E. Abdel-Rahman and A. Nayfeh, "Pendulation reduction in boom cranes using cable length manipulation," *Nonlinear Dynamics*, vol. 27, no. 3, pp. 255–269, 2002.

[7] E. Arnold, O. Sawodny, A. Hilderbrandt, and K. Schneider, "Anti-sway system for boom cranes based on an optimal control approach," in *American Control Conference*, vol. 4, Denver, CO, 2003.

[8] D. Lewis, G. G. Parker, B. Driessen, and R. D. Robinett, "Command shaping control of an operator-in-the-loop boom crane," in *American Control Conference*, Philadelphia, PA, 1998, pp. 2643–7.

[9] D. Liu, W. Guo, and J. Yi, *GA-Based Composite Sliding Mode Fuzzy Control for Double-Pendulum-Type Overhead Crane*. Berlin: Springer-Verlag, 2005, pp. 792–801.

[10] W. Guo, D. Liu, J. Yi, and D. Zhao, "Passivity-based-control for double-pendulum-type overhead cranes," in *IEEE Region 10 Annual International Conference*, Chiang Mai, Thailand, 2004, pp. D546–D549.

[11] W. Singhose and D. Kim, "Manipulation with tower cranes exhibiting double-pendulum oscillations," in *IEEE Int. Conf. on Robotics and Automation*, Rome, Italy, 2007.

[12] W. Singhose, D. Kim, and M. Kenison, "Input shaping control of double-pendulum bridge crane oscillations," *ASME J. of Dynamic Systems, Measurement, and Control*, vol. 130, no. 034504, May 2008.